Faceting at the step flow threshold in epitaxial growth on patterned surfaces

Aleksy K. Jones, Anders Ballestad, Tian Li, Michael Whitwick, Jörg Rottler, and T. Tiedje*
Department of Physics and Astronomy, The University of British Columbia, 6224 Agricultural Road, Vancouver, British Columbia, Canada V6T 1Z1

(Received 7 November 2008; revised manuscript received 7 March 2009; published 20 May 2009)

We identify a kinetic mechanism responsible for the emergence of low-angle facets in recent epitaxial regrowth experiments on patterned surfaces. Kinetic Monte Carlo simulations of vicinal surfaces show that the preferred slope of the facets matches the threshold slope for the transition between step flow and growth by island nucleation. At this crossover slope, the surface step density is minimized and the adatom density is maximized, respectively. A model is developed that predicts the temperature dependence of the crossover slope and hence the facet slope.

DOI: 10.1103/PhysRevB.79.205419 PACS number(s): 81.15.Aa, 68.55.J−, 81.15.Hi

I. INTRODUCTION

A major challenge in the field of epitaxial growth is to understand and control the relationship between macroscopic surface shapes and underlying atomic processes that create these shapes.[1] Furthermore, in semiconductor device manufacturing, regrowth on patterned substrates is commonly used as a means to control the lateral distribution of deposited material in order to synthesize optical waveguides or electron confinement structures.[2–4] Since epitaxial growth typically occurs far from equilibrium, kinetic effects can lead to rich behavior in the surface shape evolution. For example, in the case of metals, a flat surface is typically unstable against the formation of pyramidal mounds with a characteristic slope due to a tendency for adatoms (normally an isolated surface atom with no lateral bonds) to diffuse uphill.[5] An uphill diffusion bias can be caused by features of a diffusing adatom's energy landscape that tend to drive adatoms to uphill step edges over time; a well-known example is the Ehrlich-Schwoebel (ES) barrier ΔE_s (Ref. 6) that adatoms must surmount in traversing a step edge to a neighboring terrace.

In the case of GaAs (001) epitaxy, patterned surfaces become smoother during growth and there is a downhill rather than uphill diffusion bias.[7,8] Nevertheless, recent regrowth experiments show slope selection and facet formation as the surface smoothens. Ballestad *et al.*[9] demonstrate facet development during molecular beam epitaxy (MBE) growth on patterned surfaces at 580 °C. Examples of the facets are reproduced in the cross-sectional atomic force microscope images of microfabricated one-dimensional (1D) gratings in Fig. 1(a). Similar results using MBE have been observed by Kan *et al.*[10] These features have also been reported by Wixom *et al.*[11] in GaAs grown at 620 °C by metal organic chemical vapor deposition on patterned substrates. Note that the surface facets discussed here are low-angle facets, which form during growth on vicinal surfaces with surface orientations close to (001). This contrasts with earlier work on regrowth on high-angle-patterned surfaces in which both (001) and (111) crystallographic facets are exposed.[12] Here, we present an explanation for the facets observed in these experiments using kinetic Monte Carlo (kMC) simulations and simple scaling arguments.

II. RESULTS FROM EXPERIMENTS AND SIMULATIONS

The emergence of facets is readily reproduced in kMC simulations of a solid on solid model. Adatoms are deposited with a deposition rate $F=1$ ML/s onto a substrate consisting of a square lattice and undergo thermally activated hops to nearest-neighbor sites.[13] The hopping frequency can be written as $\omega=\omega_0 \exp[-(E_d+mE_b+\Delta E_s)/k_BT]$, where E_d denotes the energy barrier for the free diffusion of monomers, E_b is an additional binding energy for a monomer surrounded by m nearest neighbors, and $\omega_0=2k_BT/h\sim 10^{13}$ s^{-1} is an attempt frequency. The ES barrier ΔE_s only contributes to the hopping rate if the adatom is traversing a step edge. We employ values for the energy barriers broadly suitable for modeling MBE growth of GaAs: $E_d=1.25$ eV, $E_b=0.35$ eV, and $\Delta E_s=-0.10$ eV.[9] The negative sign for ΔE_s means that the ES barrier favors downhill migration of adatoms so that there is a net downhill current in the kMC simulations.

Figure 1 presents results for regrowth on a prepatterned surface from (a) experiment and (b) kMC simulation for direct comparison. In the simulation, a grating profile has developed facets with a well-defined slope $\pm\theta_f$ near the grating peak after deposition of 6000 monolayers. The facets grow in size and become better defined as the simulation goes on, and the general shape of the evolving facets is in agreement with the experimental results. The slope θ_f is weakly temperature dependent and decreases with increasing temperature. Figure 2 shows results from another regrowth experiment on the same substrate but in a different surface orientation and under slightly different growth conditions. Again a clear facet has become visible near the peak. These experiments are strong evidence that the effect is robust and not dependent on a specific set of growth parameters. The difference in the shape of the experimental and simulated surface shapes in Fig. 1 (simulated shapes are more square than the experiments) is caused by the fact that the smoothing rate of the simulated surface profile is lower than the experimental value. The smoothing rate in the simulation could be increased by adding an incorporation barrier that inhibits the attachment of adatoms to step edge boundaries at upper terraces. We also note that the valleys for both the simulations and the experiments are V shaped in Fig. 1 but

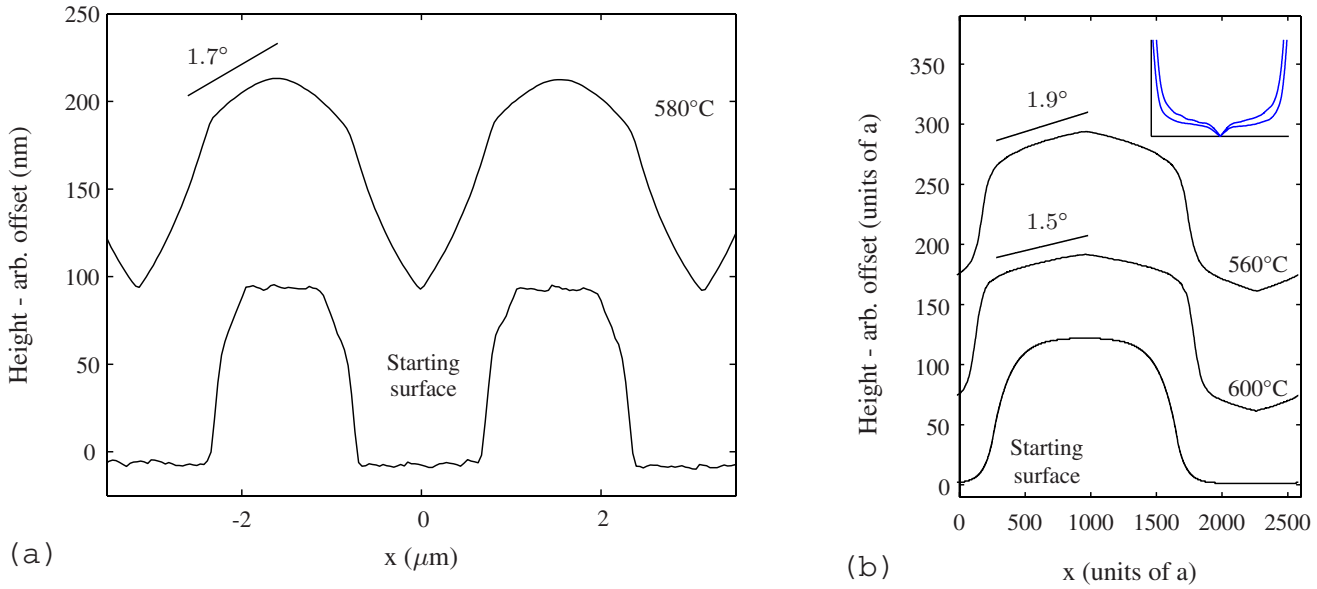

FIG. 1. (Color online) (a) Experimental atomic force microscope cross sections of 1D gratings on GaAs (001) with the [110] direction in the plane of the page. The bottom line shows the initial microfabricated grating profile before any growth has taken place. The next line is after deposition of 600 nm of GaAs at 580 °C. The straight line indicates the facet slope θ_f. (b) Grating profiles for kMC simulations on a patterned surface at two different temperatures after deposition of 6000 monolayers on a surface with 2600×600 sites. Each point in the 2D profile is an average over the 600 surface sites in the third dimension. The inset shows the profile slope in the area surrounding the grating peak at 560 (upper curve) and 600 °C (lower curve).

W shaped in Fig. 2. The physical origin of these features is discussed in earlier publications.[9,14] The small mounds in the valleys in Fig. 2 can also be expected to develop kinetic facets with the same characteristic slopes that are seen on the ridge tops.

Much effort has gone into the theory behind epitaxial regrowth on nonsingular surfaces. However, the models only address the formation of high-symmetry crystal facets based on their equilibrium interfacial properties.[15–17] The facets at θ_f we refer to in this paper are of a different physical origin and are better understood as vicinal regions of a particular slope. In order to understand their physical origin, we perform a second set of kMC simulations on vicinal surfaces, where the surface is not prepatterned but constrained to a fixed slope θ. A useful parameter is the step density S, defined as the total length of all the steps on the surface divided by the area of the surface. S has dimensions of nm^{-1} and as long as the step edges are relatively smooth, S is approximately equal to the reciprocal of the step separation. For sloping surfaces with straight step edges $S \simeq \theta/a$, where a is the lattice constant, but for ramified steps, S will be greater than this lower limit.

In Fig. 3(a) we calculate S from kMC simulations as a function of vicinal angle θ for several different temperatures under steady-state growth conditions. As one would expect, S rises linearly with θ for large values of θ. However, for $T \geq 450$ °C there is a minimum in the step density at nonzero slope $\theta_{\min}$, as reported earlier,[18] and this minimum shifts to smaller angles with increasing temperature. Figure 3(b) shows the adatom density n as a function of surface slope. We note that it has a maximum at slopes close to but slightly smaller than $\theta_{\min}$ in the temperature range of 400–600 °C studied here.

III. DISCUSSION

It has long been appreciated that a vicinal surface grows either in a step flow mode, in which all deposited adatoms attach to existing step edges, or in a nucleation dominated regime in which new steps are continuously being created by nucleation of islands.[1] The transition from step flow to island nucleation can be observed experimentally as the onset of reflection high-energy electron diffraction oscillations.[19] The lower part of the inset of Fig. 3 shows a top view of the step edges at the slope corresponding to the step density mini-

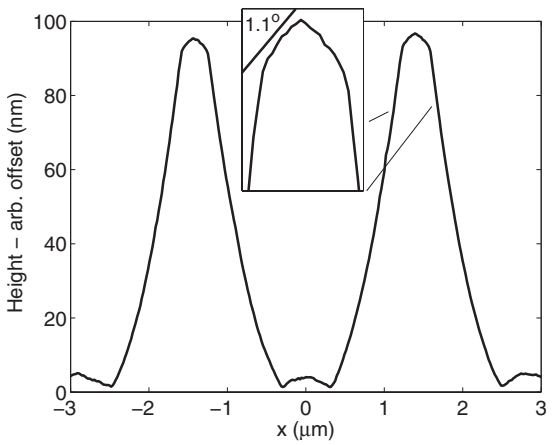

FIG. 2. Experimental atomic force microscope cross sections of 1D gratings on GaAs (110) with the $[1\bar{1}0]$ direction in the plane of the page after deposition of 200 nm of GaAs at 590 °C and a deposition rate of 0.29 ML/s. Other experimental parameters are similar to Ref. 9. The starting surface has a trapezoidal shape similar to that shown in Fig. 1(a).

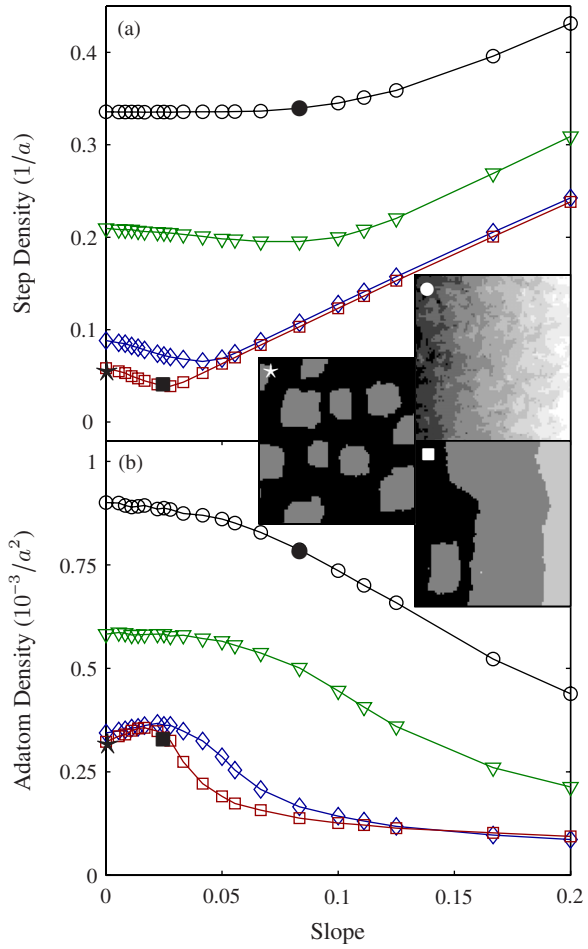

FIG. 3. (Color online) (a) Step density S and (b) adatom density n on vicinal surfaces as a function of slope for 400, 450, 550, and 600 °C (○,▽,◇,□). The inset shows one step edge pattern at 400 °C and two patterns at 600 °C at the slopes indicated by symbols in the main figure.

mum at 600 °C. This picture suggests that the growth process makes a transition from island nucleation to step flow near the slope at which the step density is minimized. It follows that at higher slopes the surface consists of a staircase of parallel steps while at lower slopes the step pattern includes closed loops surrounding monolayer islands.

Steps in a parallel configuration capture adatoms more efficiently than steps that form closed loops for the same step density. In fact, a solution of the two-dimensional (2D) diffusion equation[20] for parallel steps and steps in the form of square loops (all steps assumed to be perfectly absorbing) at the same step length per unit area gives a steady-state mean adatom density 1.7 times higher for the closed loops. Under steady growth conditions, island nucleation establishes a step density such that the adatom capture rate matches the flux of incoming adatoms. The step density required to achieve this balance will be higher with steps in the form of closed loops (inefficient capture) and lower for steps in the form of parallel lines (efficient capture). At the onset of step flow growth, the steps are in the form of parallel lines, which explains why the step density is a minimum at this condition.

In addition, Fig. 3(b) shows that at the onset of step flow growth, the mean adatom density is largest. This is because

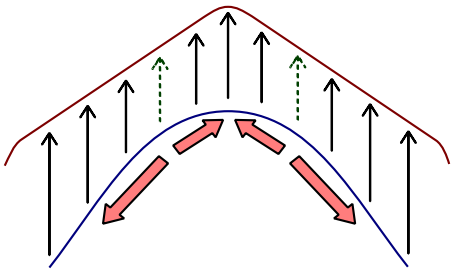

FIG. 4. (Color online) Schematic plot of facet development at the step density minimum (see text). Shaded arrows represent adatom diffusion away from areas of low S and the dashed arrows represent the areas of lowest growth rate.

the adatom density has larger spatial variations when steps are in the form of closed loops, which leads to increased island nucleation, a higher step density, and in turn to a lower adatom density. We have confirmed this interpretation numerically using idealized step edges in the form of squares and straight parallel lines.

The physical origin of the slope selection can be understood with reference to growth on a convex surface, as shown schematically in Fig. 4. The high adatom density in the region with slope corresponding to $\theta_{\min}$ will lead to lateral diffusion of adatoms to nearby areas where the adatom density is lower and the step density is higher. The lateral diffusion of adatoms away from the slope with minimum step density means that neighboring regions will grow faster, tending to expand the area with slope matching the minimum in the step density. This process will create an extended region with slope equal to $\theta_{\min}$, or in other words, a facet.[16,21]

In Fig. 5, we plot the facet slope θ_f in the regrowth simulation, along with the value of the step density minimum $\theta_{\min}$ obtained from the simulations on vicinal surfaces as a function of temperature. Remarkably, θ_f closely tracks $\theta_{\min}$ in the temperature range of 550–625 °C. Also shown is the slope

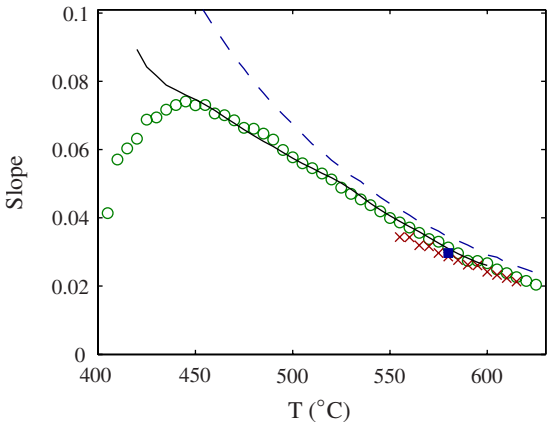

FIG. 5. (Color online) Temperature dependence of the facet slope θ_f(×) from the regrowth simulations [as shown in Fig. 1(b)], the slope at the minimum in the step density $\theta_{\min}$ (○) as determined from simulations on vicinal surfaces [Fig. 3(b)], and the experimental data point θ_f (■) from Fig. 1(a). Also shown are (- -) the reciprocal of the nucleation length at zero slope represented by $aS_0/2$, where S_0 is the step density at zero slope (see text), and (—) the threshold slope for step flow growth predicted from Eq. (2).

of the experimental facet from Fig. 1(a), which coincides with the simulated slope at the same temperature and deposition rate. However, this good agreement must be regarded as a coincidence because we have made no attempt to adjust the parameters to fit the data. Since the growth parameters are only weakly constrained by the single experimental data point, even approximate agreement between the simulation and experiment is sufficient to show that the proposed mechanism is consistent with the experimental observations. The accessible temperature range is constrained by faceting behavior and by practical considerations: at lower temperature the facet slope becomes indistinct and at higher temperature we are limited by processor time.

Having established that the preferred slope θ_f is controlled by the step density minimum $\theta_{\min}$, we now construct a model that explains the temperature dependence of $\theta_{\min}$. In order to quantitatively describe the transition between the step flow and nucleation-dominated regimes, it is natural to compare the typical spacing between vicinal steps l_s to the typical distance between nucleated islands; the latter quantity is often referred to as the nucleation length l_n.[1,22] For $l_s \ll l_n$ one expects step flow growth and for $l_s \gg l_n$, island nucleation will take place. A simple estimate for the crossover slope $\theta_{\min}$ is therefore

$$\theta_{\min} \sim a/l_n. \tag{1}$$

A first approximation to the nucleation length l_n can be obtained from S_0, the step density at zero slope. If the steps are relatively smooth, the inverse of the step density is approximately equal to the step spacing.[1] Therefore, the nucleation length can be approximated by $2/S_0$. The factor of two comes about from the fact that if steps are evenly distributed on a surface, the distance between the centers of neighboring islands will be twice the separation of the step edges. The temperature dependence of l_n has been studied previously in great detail.[22–24] Here, we have deliberately chosen an estimator for the nucleation length which is simple, experimentally accessible, and consistent with that used in the literature.

In Fig. 5 we also plot the above estimate for the step density minimum (dashed line). The slope estimated from the nucleation length agrees quite well with $\theta_{\min}$ for higher temperatures but starts to show deviations at lower temperatures. Starting at high temperature, the slope at the minimum step density first increases as the temperature decreases, then drops rapidly to zero at a critical temperature. The initial increase in slope is driven by the temperature dependence of the nucleation length which becomes progressively smaller at low temperatures. However, there is a limit to this mechanism: once l_n is smaller than the roughness of the step edges, the distinction between the parallel steps of the step flow regime and the closed-loop steps of the nucleation dominated regime is lost, and the crossover vanishes. Below this temperature $\theta_{\min}$ drops rapidly to zero, as shown in Fig. 5. The shape of the step edges in the low-temperature regime where the step edges are rough can be seen in the upper inset of Fig. 3.

A more refined interpretation of the step density minimum is also possible. In this approach, we include the roughness of the step edges explicitly and calculate the nucleation length on vicinal terraces directly. We introduce the nucleation length on a vicinal surface l_{nv}, which is calculated with separate kMC simulations in a geometry with two perfectly absorbing parallel boundaries that represent the step edges. $l_{nv}(T)$ is then taken as the separation between the boundaries where stable islands first begin to appear. In order to capture the effect of the deviation of the step edges from straight lines, we calculate the root-mean-square displacement w_{rms} of a step edge around its mean position; w_{rms} could be interpreted as an effective thickness of the step edges. The step edges are therefore effectively closer together than estimated by the average terrace spacing l_s. The transition from island nucleation to step flow growth occurs when the effective terrace spacing is equal to l_{nv} (Ref. 1) so the crossover criterion would then read $l_{nv}=c_1 l_s - c_2 w_{\mathrm{rms}}$, where $c_1=0.8$ and $c_2=2.2$ are adjustable constants determined by fitting. Solving for l_s and taking $\theta_{\min}=a/l_s$, we obtain

$$\theta_{\min} = \frac{a}{c_1 l_{nv} + c_2 w_{\mathrm{rms}}}. \tag{2}$$

This expression provides an excellent approximation of the step density minimum, as shown in Fig. 5, where we plot Eq. (2) as a function of $1000/T$ (solid line). Note that the improved model also captures the curvature in the temperature dependence of the step density minimum at low temperatures where the model based on the zero slope step density fails. The good agreement is a strong indication that our interpretation captures all relevant physics of the step density minimum.

The temperature dependence of the facet slope contains information about island nucleation through its relationship to the step density. According to nucleation theory,[1] the step density is controlled by the formation of stable nuclei on the surface and depends on growth rate F and adatom diffusion constant D according to $S \sim (F/D)^{(x/2x+4)}$, where x is the size of a critical nucleus. We can use this relation and the data in Fig. 5 to estimate the size of the critical nucleus. The temperature dependence of the step density on the high-temperature end of Fig. 5 corresponds to an activation energy of 0.42 eV. From this value and the known activation energy for terrace diffusion (1.25 eV) we conclude that the critical nucleus size is $x=4$.

Although we do not have experimental measurements of the slope at the minimum step density, we can estimate the zero slope step density S_0 from atomic force microscope images. According to the above argument, $aS_0/2$ should be approximately equal to the facet slope. Indeed this turns out to be the case. At a growth temperature of 590 °C, the step density is found to be 0.079 nm^{-1}.[25] Using a step height $a=0.27$ nm, appropriate for GaAs (001) surfaces, we find $aS_0/2=0.6°$. This value can be compared with the facet slopes indicated by the straight lines in Figs. 1(a) and 2, which have a slope of 1.7° and 1.1°. The slope of similar facets in Ref. 10 was found to be about 1° for a sample grown under comparable conditions (585 °C, 1 ML/s). In addition, we note that the grating patterns in Figs. 1(a) and 2 are oriented orthogonally with respect to each other. In Fig. 1(a) the relevant surface step spacing is perpendicular to the

slow surface diffusion direction on GaAs (100) ([110] direction) while in Fig. 2 the relevant step spacing is perpendicular to the fast-diffusion direction on GaAs (100). Higher surface mobility in the $[1\bar{1}0]$ direction means that the atomic step spacing should be larger in this direction; therefore we can expect the kinetic facet slopes to be lower for the grating in Fig. 2. Taking into account the surface anisotropy, the uncertainties in the experimental values of the step densities, and likely variations in the growth conditions, the observed level of agreement between the model and the experiments (0.6° compared with 1°, 1.7°, and 1.1°) is entirely reasonable.

IV. CONCLUSION

In conclusion, we have discovered a mechanism for slope selection in epitaxial crystal growth at the crossover between step flow and island nucleation. This kinetically defined slope leads to a characteristic facet slope which has been identified both in kinetic Monte Carlo simulations and in several epitaxial regrowth experiments on patterned GaAs substrates. However, the processes behind the slope selection mechanism are completely general and do not depend on the specifics of the GaAs system.

ACKNOWLEDGMENT

We thank the Natural Sciences and Engineering Research Council of Canada (NSERC) for financial support.

*Present address: Department of Electrical and Computer Engineering, University of Victoria, Victoria, British Columbia, Canada V8W 3P6.

[1] A. Pimpinelli and J. Villain, *Physics of Crystal Growth* (Cambridge University Press, Cambridge, 1998).
[2] E. Kapon, D. M. Hwang, and R. Bhat, Phys. Rev. Lett. **63**, 430 (1989).
[3] I. Tamai, T. Sato, and H. Hasegawa, Jpn. J. Appl. Phys., Part 1 **44**, 2652 (2005).
[4] P. Poole, G. Aers, A. Kam, D. Dalacu, S. Studenikin, and R. Williams, J. Cryst. Growth **310**, 1069 (2008).
[5] T. Michely and J. Krug, *Islands, Mounds and Atoms* (Springer, New York, 2004).
[6] G. Ehrlich and F. Hudda, J. Chem. Phys. **44**, 1039 (1966); R. L. Schwoebel and E. J. Shipsey, J. Appl. Phys. **37**, 3682 (1966).
[7] A. Ballestad, B. J. Ruck, J. H. Schmid, M. Adamcyk, E. Nodwell, C. Nicoll, and T. Tiedje, Phys. Rev. B **65**, 205302 (2002).
[8] V. R. Coluci, M. A. Cotta, C. A. C. Mendonça, K. M. I.-Landers, and M. M. G. de Carvalho, Phys. Rev. B **58**, 1947 (1998).
[9] A. Ballestad, T. Tiedje, J. Schmid, B. Ruck, and M. Adamcyk, J. Cryst. Growth **271**, 13 (2004).
[10] H. C. Kan, R. Ankam, S. Shah, K. M. Micholsky, T. Tadayyon-Eslami, L. Calhoun, and R. J. Phaneuf, Phys. Rev. B **73**, 195410 (2006).
[11] R. Wixom, L. Rieth, and G. Stringfellow, J. Cryst. Growth **269**, 276 (2004).
[12] F. Grosse and R. Zimmermann, J. Cryst. Growth **212**, 128 (2000).
[13] J. P. DeVita, L. M. Sander, and P. Smereka, Phys. Rev. B **72**, 205421 (2005).
[14] T. Tiedje and A. Ballestad, Thin Solid Films **516**, 3705 (2008).
[15] V. Shenoy, A. Ramasubramaniam, and L. Freund, Surf. Sci. **529**, 365 (2003).
[16] M. Ohtsuka, J. Cryst. Growth **205**, 112 (1999).
[17] W. Braun, V. M. Kaganer, A. Trampert, H.-P. Schönherr, Q. Gong, R. Nötzel, L. Däweritz, and K. H. Ploog, J. Cryst. Growth **227-228**, 51 (2001).
[18] A. Ballestad and T. Tiedje, Phys. Rev. B **74**, 153405 (2006).
[19] T. Shitara, D. D. Vvedensky, M. R. Wilby, J. Zhang, J. H. Neave, and B. A. Joyce, Phys. Rev. B **46**, 6815 (1992).
[20] W. K. Burton, N. Cabrera, and F. C. Frank, Philos. Trans. R. Soc. London Ser. A **243**, 299 (1951).
[21] S. Li, Q. Xiang, D. Wang, and K. L. Wang, J. Cryst. Growth **164**, 235 (1996).
[22] J. Evans, P. Thiel, and M. Bartelt, Surf. Sci. Rep. **61**, 1 (2006).
[23] C. Ratsch, A. Zangwill, P. Smilauer, and D. D. Vvedensky, Phys. Rev. Lett. **72**, 3194 (1994).
[24] C. Ratsch and J. A. Venables, J. Vac. Sci. Technol. A **21**, S96 (2003).
[25] M. B. Whitwick, T. Tiedje, and T. Li, J. Cryst. Growth **310**, 3192 (2008).